Thermodynamic Properties of Stereoregular Poly(methyl methacrylate)

James M. O'Reilly,* Harvey E. Bair,† and Frank E. Karasz‡

General Electric Research and Development Center, Schenectady, New York 12345.
Received August 21, 1980

ABSTRACT: Specific heat data for isotactic, atactic, and syndiotactic PMMA from 80 to 445 K are reported. The specific heats of the three polymers are monotonic functions of temperature and are the same within 1% from 80 to 300 K. Glass transition temperatures of 318, 378, and 388 K are observed for isotactic, atactic, and syndiotactic PMMA, respectively, with small differences in ΔC_p. In the liquid the isotactic polymer has a slightly higher specific heat. Only the isotactic polymer could be prepared in the crystalline state by solvent treatment and yielded crystals with a maximum melting point of 435 K. From the calculated entropy of the crystalline and amorphous isotactic polymer, a residual entropy at T_g of 2.5 eu is found. Extrapolation of ΔS_g to zero leads to $T_g - T_2 = 33$ K and $T_2 = 285$ K. In addition, the calorimetrically determined difference in entropy between PMMA stereoisomers was found to be 3 eu. The calculated conformational contributions to this difference were about 0.5 eu from rotational isomeric state calculations and volume effects. Thus additional intermolecular and/or intramolecular factors contribute to the entropy.

Introduction

The specific heat and derived thermodynamic data for isotactic, atactic, and syndiotactic PMMA are presented. Differences in thermal properties are investigated from low temperature through the glass transition temperature and into the liquid temperature regimes. A primary emphasis of these studies was to investigate the effect of stereoregularity upon the molecular motion in the glassy state, the change in specific heat at the glass transition temperature, and the entropy of the polymer liquid. The entropy measurements provide a test of the Gibbs–DiMarzio[1] theory of the glass transition and a comparison with entropy data on polypropylene[2] and polystyrene.[3]

Experimental Section

Samples. The isotactic sample was synthesized by the method of Goode.[4] Two samples of different fractional crystallinities (0.18 and 0.40 from the heat of melting) were prepared by swelling the isotactic polymer in heptanone. Syndiotactic polymer was generously supplied by Rohm and Haas Co. Atactic polymer, polymerized in sheet form, was obtained from Rohm and Haas Co. Note that the latter commercial polymer has a significant component of syndiotactic triads (Table I).

Measurements of the intrinsic viscosity in $CHCl_3$ yielded the molecular weight data in Table I. In addition, triad sequences obtained from proton NMR are listed in Table I.

Calorimetry. The calorimeter, modified to allow measurements in a temperature range of 14 to 600 K, was of conventional adiabatic design and has been described previously.[5] The samples, sealed under a few centimeters pressure helium, were typically heated at a rate between 1 and 15 K h^{-1}. An intermittent heating technique was used, with intervals ranging from 2 to about 10 K. Equilibration times were normally about 20 min but increased sharply in the vicinity of transitions. The weights of the samples used were 20–30 g. The precision of the apparatus had previously been assessed by a determination of the heat capacity of a standard sample of alumina.[5] For the present measurements, we estimate our errors in the heat capacity to average ±0.2% up to about 400 K, with a possible rise to ±0.4% at the highest temperatures used.

X-ray Diffraction. X-ray diffraction measurements were obtained in reflection with a GE XRD-5 diffractometer from pressed samples (~1 mm thick). The scattering intensity for the crystalline samples was not sufficiently well defined to warrant quantitative analysis of percent crystallinity.[3] Qualitative interpretations of the X-ray data are given in the text.

Table I

sample	$[\eta]$,[a] dL/g	M_w	fraction of triads by ^{1}H NMR iso	hetero	syndio
isotactic	0.89	6.1×10^5	0.95	0.05	0
atactic	0.44	9×10^4	0.06	0.37	0.56
syndiotactic	0.47	9.8×10^4	0.10	0.20	0.70

[a] $CHCl_3$, 25 °C.

Table II
Syndiotactic PMMA

T_{av}, K	C_p, J deg^{-1} g^{-1}	T_{av}, K	C_p, J deg^{-1} g^{-1}
81.01	0.473	292.93	1.367
87.64	0.506	307.12	1.425
94.82	0.543	321.26	1.478
101.20	0.576	332.82	1.522
107.37	0.608	343.95	1.566
113.83	0.638	353.80	1.606
120.50	0.672	361.94	1.640
128.17	0.708	368.61	1.674
136.38	0.744	373.65	1.702
143.59	0.776	377.54	1.725
150.73	0.804	380.87	1.735
159.19	0.839	383.90	1.767
168.11	0.875	386.69	1.806
176.21	0.906	389.31	1.848
183.59	0.932	391.94	1.918
192.41	0.968	394.50	2.026
202.93	1.006	397.01	2.130
213.84	1.048	399.81	2.150
221.54	1.085	404.68	2.116
228.11	1.146	412.34	2.146
237.25	1.153	420.82	2.152
245.52	1.168	429.89	2.208
254.70	1.210	438.29	2.238
267.44	1.260	445.97	2.259
278.86	1.304	454.01	2.302
285.20	1.334	462.15	2.313

Results and Discussion

Atactic and Syndiotactic PMMA. The heat capacities of a-PMMA and s-PMMA differ by less than 0.5% from 80 to 300 K as shown in Figure 1. Tables II and III contain the measured heat capacities at the midpoint of the temperature range. From 80 to 150 K, the C_p curve shows curvature but becomes linear with temperature above 150 K. There is no evidence of any bumps or

* To whom correspondence should be addressed at Eastman Kodak Research Laboratories, Rochester, NY 14650.
† Bell Laboratories, Murray Hill, NJ 07974.
‡ University of Massachusetts, Amherst, MA 01003.

0024-9297/82/2215-1083$01.25/0

Table III
Atactic PMMA

T_{av}, K	C_p, J deg^{-1} g^{-1}	T_{av}, K	C_p, J deg^{-1} g^{-1}
81.33	0.474	326.48	1.506
88.59	0.516	336.45	1.548
97.30	0.558	346.41	1.588
106.33	0.604	354.54	1.622
113.85	0.641	360.16	1.668
119.94	0.672	364.13	1.707
126.38	0.701	367.14	1.733
132.90	0.731	370.36	1.750
138.05	0.752	373.99	1.795
142.67	0.773	377.67	1.876
150.26	0.806	380.61	1.957
158.06	0.837	382.72	2.023
165.98	0.868	384.92	2.050
175.48	0.904	387.20	2.065
183.94	0.940	389.83	2.075
191.97	0.967	393.21	2.086
201.51	0.999	356.99	1.634
211.77	1.044	365.52	1.713
222.19	1.100	371.22	1.757
232.51	1.137	374.98	1.849
239.57	1.150	379.09	1.978
245.93	1.177	383.12	2.069
254.96	1.215	385.70	2.058
263.12	1.247	389.76	2.073
271.36	1.280	395.51	2.091
280.52	1.315	402.23	2.112
289.69	1.358	410.97	2.143
298.59	1.395	418.47	2.175
307.42	1.428	426.61	2.196
316.86	1.473	437.14	2.232

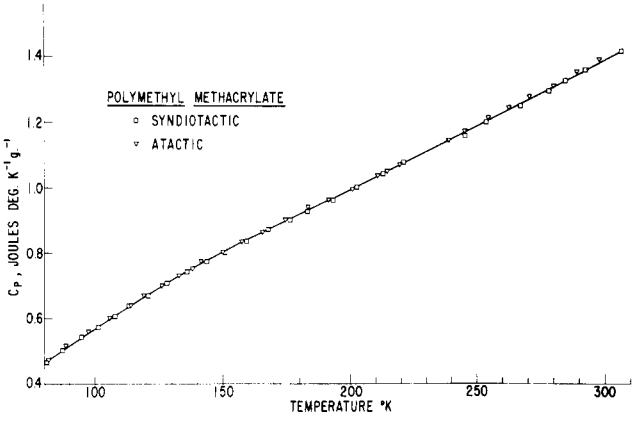

Figure 1. Specific heat of atactic and syndiotactic PMMA from 80 to 300 K.

transitions from 80 to 300 K. Sochava and Trapeznikova[6] have reported two bulges in C_p, one between 60 and 130 K and another between 130 and 180 K. Besides the difference in shape of the C_p curves, the absolute values of C_p do not agree very well. Their values are from 3 to 10% lower than ours from 150 to 260 K, and their accuracy is reported to be about 1%. It seems unlikely that these differences could be due to sample diferences, but it is difficult to be certain since no sample characteristics are given. In any event, it is clear that the reported bumps are not characteristic of PMMA and, therefore, should not be used as evidence for specific molecular motion in PMMA.

Evidence for different molecular motions in PMMA can be summarized as follows: (a) ester methyl groups rotate at 42 K (NMR and mechanical measurements);[7,8] (b) α-methyl rotation is frozen in below 100 K (NMR);[8] (c) carbomethoxy group motion occurs above 270 K (mechanical and electrical measurements);[7] (d) large-scale segmental motion occurs above T_g (370 K).[7]

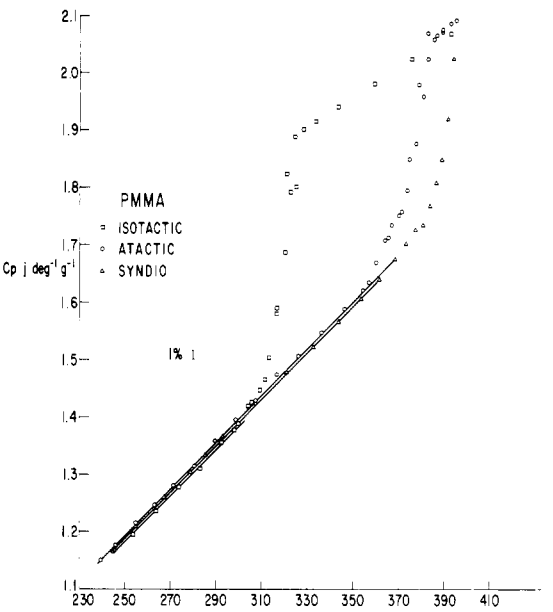

Figure 2. Specific heat in glass transition region of isotactic, atactic, and syndiotactic PMMA.

Since no abrupt changes occur in C_p between 80 and 300 K, we conclude that the motions b and c do not occur abruptly but rather continuously. If a methyl group is undergoing torsional oscillation, it will contribute R or 2 cal/(mol K) to C_p. On the other hand, a freely rotating methyl group will contribute $R/2$ or 1.0 cal/(mol K). In PMMA, a torsional oscillator would contribute 10% to the total C_p at 150 K, while a free rotor would contribute 5%. A gradual transition from oscillation to rotation would be accompanied by a decrease in C_p of $R/2$ cal/(mol K). The reason that this decrease is not observed in the experimental C_p curve is that it occurs over a wide temperature range and the effect is somewhat masked by the increased contribution of other mechanisms (acoustical and optical modes), which more than compensate for the drop-off of internal rotation modes. In principle, one could theoretically calculate the contribution of the various modes and show that the internal rotations do contribute to C_p.[9]

At about 360 K, which is just 10 K below T_g, there is an upturn in C_p for the atactic sample (Figure 2). Experience with other polymers indicates that this upturn is not usually observed near the glass transition. A similar upturn of smaller magnitude occurs below T_g of the syndiotactic sample. An isotactic sample also shows a very small upturn just below T_g (378 K). These increases are not considered to be associated with the process that gives rise to the mechanical and dielectric losses that occur below T_g in the stereoregular samples.[7] Heat capacity measurements, like volumetric measurements, detect transitions at lower temperatures than mechanical or electrical measurements because they are effectively lower frequency or longer scale measurements. The upturns could be associated with microheterogeneities in stereoregularity that lead to slightly lower T_g's. However, there is no independent evidence from NMR or IR measurements that supports this speculation. No other explanation for the upturn is available at this time.

Kovacs and Wittman[10] have made dilatometric measurements on these same PMMA samples. They find several transitions below T_g that are greater in magnitude at other temperatures and do not correspond to the minor effects in C_p reported here. In the atactic sample, a break in the volume curve is observed at 273 and at 343 K, whereas our C_p curve is smooth within experimental error.

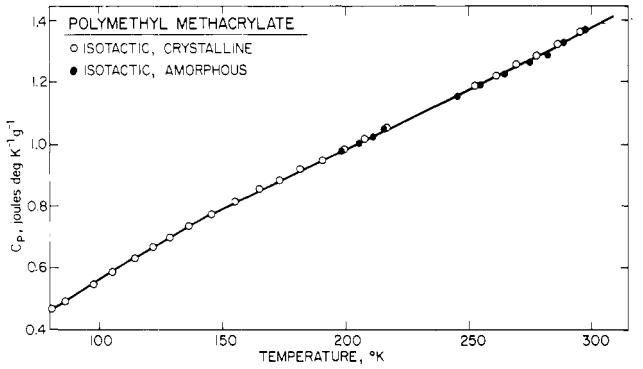

Figure 3. Specific heat of isotactic PMMA semicrystalline (18%) and amorphous samples.

There is no evidence in the dilatometric measurements of the upturn observed in C_p at 360 K. Figure 2 shows this region on an expanded scale and demonstrates that the curves are smooth: no abrupt changes of the order of 1% are visible up to 350 K. These results seem to indicate that accurate measurements of expansivity and specific heat are sensitive in different ways to the molecular motion. Theoretically, the expansion coefficient is sensitive to the anharmonicity of the potential functions while specific heat is determined mainly by harmonic terms. This behavior is in contrast to the usual similarity of thermal and volumetric measurements in studying melting transitions at T_m through ΔH_f and ΔV_f.

Simha and co-workers[11] have shown that many polymers exhibit changes in expansivity at low temperatures. It does appear that the expansion coefficient measurements show changes that are not observed by other methods. In many cases, the specific heat data are not available for comparison for all these polymers. The exact reasons for these differences should be sought, for they may give important insight into the structure and properties of solid polymers.

The change of C_p at T_g for a-PMMA and s-PMMA is typical of amorphous polymers except for the upturn at the onset of T_g previously mentioned. A slight peak in s-PMMA was due to the inadvertent annealing overnight of the sample below T_g before proceeding with the measurements through T_g the following day. This enthalpic relaxation phenomenon is well understood[12,13] but is frequently misinterpreted as due to crystallinity. Taking T_g as the temperature of the midpoint in the C_p curve defined by the linear liquid C_p curve and the linear glass curve yields T_g = 376 and 389 K, respectively, for a-PMMA and s-PMMA. There was no evidence of any melting or recrystallization phenomena up to 460 K (Figure 3) in syndiotactic or atactic PMMA, which is consistent with the appearance of only amorphous halos in the X-ray data.

Isotactic PMMA. There are two series of runs with i-PMMA and each series included two temperature cycles. The first series (I) of measurements was on the dried powder (~18% crystalline from the heat of melting based upon ΔH_f equal to 96 J/g) and extended from 80 to 440 K. Upon slow cooling from the melt, the sample did not recrystallize and, therefore, the glass transition of the amorphous polymer could be studied on the second heating (300–440 K). In the second series (II), the sample from the first series was crystallized in warm heptanone for 1 week, dried, and loaded into the calorimeter. This sample was studied from 80 to 440 K and was estimated to be approximately 40% crystalline from the heat of melting. Upon cooling, no crystallization occurred and the sample was remeasured in the amorphous state from 200 to 400 K. The measured values of the heat capacities are tabulated in Tables IV and V.

Table IV
Isotactic PMMA (Crystalline Fraction ~0.18)

T_{av}, K	C_p, J deg^{-1} g^{-1}	T_{av}, K	C_p, J deg^{-1} g^{-1}
83.24	0.482	335.66	1.860
89.56	0.512	343.73	1.888
97.36	0.552	352.63	1.903
102.98	0.579	361.60	1.912
108.25	0.607	370.46	1.673
116.32	0.650	378.90	1.862
123.86	0.683	387.37	1.917
130.76	0.714	392.82	1.651
138.14	0.746	397.75	2.091
145.70	0.779	406.02	2.446
153.19	0.812	411.26	3.084
160.09	0.841	413.92	3.258
167.39	0.871	416.50	3.495
175.24	0.901	419.19	3.554
182.91	0.929	421.91	3.148
190.75	0.956	424.35	2.682
198.18	0.988	426.59	2.417
206.08	1.018	428.97	2.190
215.04	1.052	431.53	2.178
221.91	1.091	435.31	2.177
226.50	1.146	439.97	2.191
231.20	1.125	298.16	1.378
237.35	1.141	304.42	1.419
245.10	1.166	309.29	1.445
253.50	1.195	313.34	1.504
263.54	1.237	317.04	1.588
273.41	1.278	320.96	1.823
282.94	1.310	324.73	1.888
292.19	1.356	328.15	1.899
299.67	1.388	333.72	1.913
305.83	1.425	343.76	1.939
311.48	1.465	359.50	1.980
316.61	1.580	376.18	2.024
320.32	1.687	393.08	2.067
322.79	1.792	412.39	2.114
325.26	1.801	429.17	2.158
327.85	1.834	439.21	2.208
330.68	1.838		

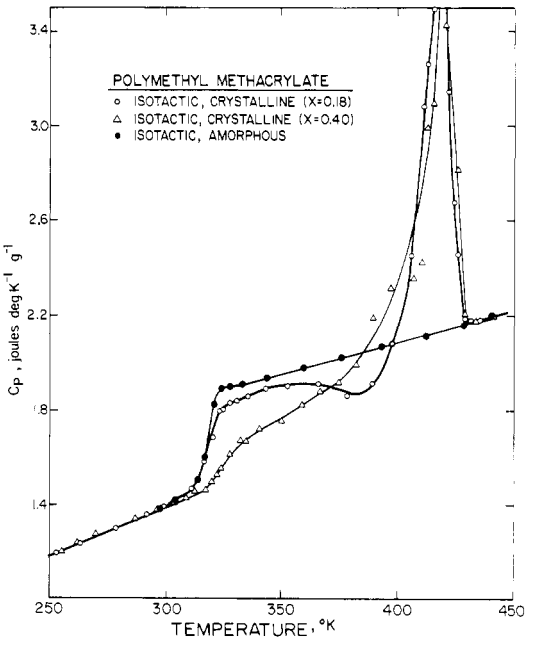

Figure 4. Specific heat of isotactic PMMA in the glass transition region, and crystal melting range for the semicrystalline and amorphous samples.

In the first series, the C_p of i-PMMA is very slightly less than the C_p of a-PMMA and s-PMMA and is a smooth function of temperature from 80 to 300 K (Figure 4). At the glass transition (319 K), the increase in C_p is characteristic of a partially crystalline sample (relative to the

Table V
Isotactic PMMA (Crystalline Fraction ~0.40)

T_{av}, K	C_p, J deg^{-1} g^{-1}	T_{av}, K	C_p, J deg^{-1} g^{-1}
80.59	0.472	407.66	2.359
86.08	0.498	410.22	2.422
91.61	0.521	412.73	2.980
97.66	0.554	415.31	3.104
105.54	0.594	417.83	2.918
114.43	0.637	420.11	3.423
122.05	0.675	422.70	3.787
128.57	0.707	425.70	2.818
136.54	0.742	428.89	2.233
145.68	0.785	434.17	2.174
155.36	0.824	441.02	2.198
165.48	0.866	199.49	0.997
173.77	0.895	206.31	1.023
182.28	0.932	211.86	1.043
191.15	0.963	217.02	1.067
200.00	1.000	224.90	1.150
208.21	1.034	233.72	1.157
216.28	1.066	239.71	1.158
225.15	1.152	246.05	1.173
233.25	1.164	255.45	1.207
242.69	1.171	265.44	1.245
253.35	1.203	275.59	1.282
262.23	1.236	282.86	1.306
270.30	1.272	289.73	1.346
278.29	1.299	298.35	1.384
286.99	1.337	304.21	1.413
296.52	1.379	308.84	1.431
304.15	1.397	313.67	1.484
309.15	1.442	317.29	1.515
312.71	1.453	319.96	1.533
315.06	1.476	322.71	1.795
317.47	1.477	325.11	2.028
319.93	1.492	327.37	1.954
322.35	1.530	329.88	1.909
324.92	1.555	333.25	1.926
328.12	1.607	339.31	1.933
331.33	1.637	348.09	1.955
334.69	1.672	356.85	1.980
328.04	1.615	363.73	1.995
332.68	1.673	371.95	2.022
340.57	1.726	380.04	2.036
349.91	1.756	389.07	2.061
358.61	1.826	400.31	2.091
366.64	1.887	411.94	2.120
374.58	1.922	423.23	2.150
382.00	1.991	431.90	2.171
389.52	2.189	439.36	2.182
397.07	2.314	447.07	2.200
403.99	3.991		

second run) as shown in Figure 4. Slow cooling produced a completely amorphous sample. Reheating this sample yielded a ΔC_p of 0.404 J deg^{-1} g^{-1}. As expected, the liquid C_p above T_g agrees with the extrapolated C_p of the liquid above T_m. The observed ΔC_p (0.336 J deg^{-1} g^{-1}) of the semicrystalline sample and ΔC_p (0.404 J deg^{-1} g^{-1}) observed for the 100% amorphous sample lead to an estimate of 16% crystallinity. About 50 K above T_g, some recrystallization occurs with the evolution of heat and leads to an apparent decrease in C_p with increasing temperature. At higher temperatures, extensive melting occurs and the apparent C_p rises abruptly. The point where the last vestige of crystallinity vanishes is denoted as T_{max} and occurs at 430 K. The heat of melting for this sample was determined from the actual heat required to heat the sample from 340 to 440 K minus the amount of heat associated with crystallization between 340 and 390 K and calculated from the area that falls below a smooth curve drawn between 340 to 440 K. This procedure leads to a heat of melting that refers to the sample as loaded into the calorimeter since the small increase due to recrystallization is excluded by this technique. A heat of melting of 18.0 J/g (4.30 cal/g) was found.

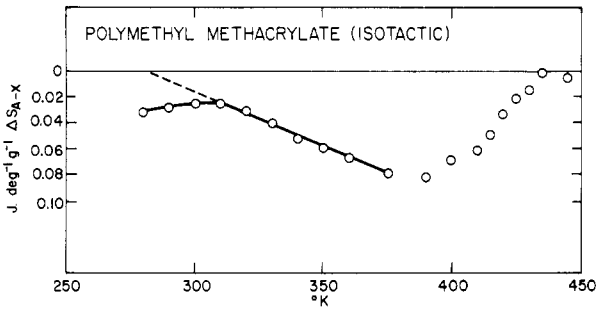

Figure 5. Entropy difference between amorphous and crystalline samples of isotactic PMMA. Extrapolated value of T_2 = 285 K.

The second series was almost indistinguishable from the first series from 80 to 300 K since the crystallinity has only a small effect on C_p in this temperature range. All the C_p results of series II were corrected by a factor of 1.01 in order to make the C_p's of these liquid samples above 320 K the same as those for the previously quenched sample from series I. This correction was attributed to an error in the calorimetric corrections due to tare weights and possibly due to a small amount of residual heptanone. At 330 K, the glass transition occurs for this semicrystalline sample, but the observed T_g is more than 10 K higher than for the previous samples. In addition, the magnitude of ΔC_p is reduced more than expected from the observed crystallinity based on its heat of melting (see Figure 4), assuming a two-phase model. The deviation of ΔC_p from two-phase behavior has been observed many times[14] and discussed previously.[15] The increase in T_g with crystallinity has been observed,[16,17] but is somewhat unusual and difficult to measure unambiguously. It is well-known that the presence of crystallites can act as physical cross-links that reduce the number of conformations and prevent the polymer from assuming its liquid-like specific heat.

At higher temperatures there was no evidence of recrystallization, only melting of crystals with the absorption of heat. The maximum melting point is the same as that found for the previous sample. The heat of melting, relative to the dashed line in Figure 4, is 40.3 J/g (9.64 cal/g). To find relative values of crystallinity in the absence of any heat of fusion data, we have assumed that the heat of fusion of i-PMMA was 96 J/g (22.9 cal/g). This value was arrived at by considering the heats of melting and ΔC_p and X-ray data of the two samples. Recent measurements[18] suggest a value of 48 J/g (12 cal/g), which appears low relative to the present results. The conclusions are in no way affected by this assumption, although the magnitudes of the calculated results are affected. In any case, these results can be corrected when more accurate values ΔH_f become available. With this assumption, the series I sample was 18% crystalline and the series II sample was 40% crystalline.

Upon rerunning the now amorphous sample, we obtained results identical with those of the second cycle of series I. There is a minor enthalpic relaxation effect at T_g, again because the sample was held overnight just below T_g. This resulted in a peak in C_p at T_g and a slightly higher transition temperature.

Residual Entropy. The entropies of each sample can be calculated from summed $C_p/T\Delta T$ increments. The excess entropy of the supercooled liquid relative to that of the crystal (ΔS_g) can be evaluated from the entropies derived from the C_p data. Results of this calculation are shown in Figure 5 for the series II sample. A residual entropy of 0.04 J deg^{-1} g^{-1} is found for the 40% crystalline sample, which would lead to a value of 0.10 J deg^{-1} g^{-1} or

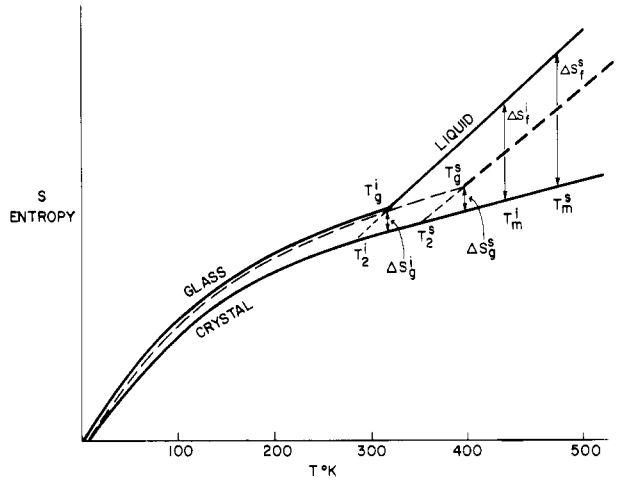

Figure 6. Schematic representation of entropy of syndiotactic and isotactic PMMA in crystalline, glassy, and liquid states.

2.5 eu/mol for a completely crystalline polymer.

$\Delta S_g(T)$ was found from the equation

$$\Delta S_g(T)_{iso} = \{S_a(T) - S_x(T)\}_{iso} \quad (1)$$

and implicity equating the entropies of the amorphous and crystalline samples in the melt above T_m. The terms $S_a(T)$ and $S_x(T)$ are obtained from the summation of the measured heat capacities of the amorphous and semicrystalline isotactic polymers divided by the absolute temperature. $\Delta S_g(T)$ is shown as a function of temperature for the semicrystalline isotactic polymer in Figure 5. Extrapolation of $\Delta S_g(T_2) = 0$ leads to $T_2 = 285$ K and $T_g - T_2 = 33$ K.

A thermodynamic theory of the glass transition for polymers by Gibbs and DiMarzio[1] has received support from thermodynamic measurements on atactic and isotactic polypropylene[2] and polystyrene.[3] In this work the central idea of Gibbs and DiMarzio (G–D) is that the excess configurational entropy of the supercooled liquid relative to that of the crystal is frozen in at T_g because the time required for equilibration becomes many orders of magnitude greater than the experimental time. G–D predict that if the supercooling would continue, a second-order thermodynamic transition would occur at T_2 aand ΔS_g would vanish at this temperture. Assuming that the entropy of the liquid atactic polymer was equal to that of the liquid isotactic polypropylene polymer, T_2 was found to be 53 ± 20 °C below T_g. In polystyrene, $T_g - T_2$ was found to be 81 ± 15 °C. Although $T_g - T_2$ is smaller than the results for polypropylene and polystyrene, this result is within the experimental uncertainties in the usually accepted value of $T_g - T_2$ (50 K).

In the absence of a crystalline sample of syndiotactic PMMA, the residual entropy, $\Delta S_g(T_g)_{syn}$, could not be evaluated experimentally. To estimate the difference in entropy of the liquid isotactic and syndiotactic polymers, we will assume that $\Delta S_g(T_g)_{syn} = \Delta S_g(T_g)_{iso}$. This assumption and its consequences are illustrated in Figure 6. The specific heats of the liquid stereoregular polymers differ only slightly and therefore isotactic PMMA has a higher entropy than syndiotactic PMMA. From the summations of $C_p\Delta T/T$, a difference in entropy between isotactic and syndiotactic PMMA at 400 K of 3.0 eu is found. The higher entropy in the isotactic PMMA may be due to a higher conformational entropy and/or a higher configurational entropy.

The conformational contribution to the entropy can be estimated from rotational isomeric state (RIS) calculations. When conformational energies and statistical weight parameters that gave the best fit to chain dimensions were used,[19] the RIS model yielded entropies[20] of $\Delta S_{conf_{iso}} = 1.13$ eu/backbone bond or 2.26 eu/mol and $\Delta S_{conf_{syn}} = 0.96$ eu/backbone bond or 1.92 eu/mol at a temperature of 400 K. Thus, the difference in conformational entropy between the isotactic and syndiotactic polymers is 0.34 eu/mol. However, this calculation refers to pure tactic polymers, whereas the experimental entropies are for PMMA polymers containing 95% isotactic and 70% syndiotactic triads. If the tacticity of the polymers used in the RIS calculations had been the same as that of the actual materials used in the C_p experiments, only a small reduction in the value of the entropy difference would have been expected.[19] Another contribution to the entropy could be due to the differences in specific volume of the polymer liquids. However, the specific volume data[10] show a difference of less than 0.5%, which taken with $(\partial S/\partial V)_T = -(\partial P/\partial T)_V = \alpha/\beta$ (expansivity/compressibility) leads to an entropy difference of 0.2 eu. The sum of both of the calculated contributions to the entropy difference of PMMA isomers is about 0.5 eu/mol. This is significantly less than the experimentally determined entropy difference of 3 eu/mol based on our C_p measurements. Thus, the thermodynamic results indicate that entropy differences between the stereoisomers are of the order of 2 eu greater than the calculated conformational contributions that are due to intramolecular and intermolecular factors.

A similar conclusion can be reached by considering the conformational energies of $\Delta H_{iso} = 700$ cal/mol and $\Delta H_{syn} = 2000$ cal/mol determined from Fourier transform infrared spectroscopy.[21] Using a two-state independent rotational state approximation that is appropriate to the FT IR results, we find the conformational entropies are $\Delta S_{conf_{iso}} = 2.70$ eu/mol and $\Delta S_{conf_{syn}} = 1.60$ eu/mol. These results are not significantly different from the RIS calculations and add credence to the conclusion that other factors contribute to the residual entropy. In examining our starting assumptions, we find that if $\Delta S_g(T_g)_{iso}$ were less than $\Delta S_g(T_g)_{syn}$, then the entropy differences in the liquid would be smaller.

Conclusions

Even with these extensive thermodynamic data, we have not been able to define conclusively the cause for the differences in glass temperature of the stereoregular PMMA. However, the primary factors are conformational entropy and configurational entropy associated with chain packing, which contributes to the excess entropy frozen in at T_g.

Another approach, due to Goldstein,[22] suggests that changes in configurational entropy occur below T_g because of changes in vibrational frequencies, molecular motion, and anharmonic effects. While all of these effects are possible, the effects in polymer glasses are not considered to be as large as they may be in small-molecule glasses. The specific heat data of Chang,[23] which show that $\Delta S_g(0\text{ K})/\Delta S_g(T_g)$ is 0.4–0.8 has been used by Goldstein to suggest that significant configurational entropy changes occur below T_g. For polystyrene (isotactic) and PMMA (isotactic), the difference in the specific heat between the crystal and glass is less than 0.5%; therefore, the loss of configurations in the glass is not significantly different from that in the crystal for these polymers. In addition, the specific heat differences between the isotactic, syndiotactic, and atactic glasses are less than 0.2% from 80 to 300 K, although there are larger differences at T_g and above. The small differences between stereoregular PMMA glasses suggest to us that the configurational changes below T_g are small.

Thus the major differences in glass temperature are attributed to differences in conformational entropies due to differences in conformational energies and configurational entropies associated with the packing of chains in the liquid.

Acknowledgment. We are grateful to A. E. Tonelli for making the entropy calculations based on the RIS model and discussing those results with us.

References and Notes

(1) Gibbs, J. H.; DiMarzio, E. A. *J. Chem. Phys.* **1958**, *28*, 373.
(2) Passaglia, E.; Kevorkian, H. *J. Appl. Phys.* **1965**, *34*, 90.
(3) Karasz, F. E.; Bair, H. E.; O'Reilly, J. M. *J. Phys. Chem* **1965**, *69*, 2657.
(4) Fox, T. G.; Garret, B. S.; Goode, W. E.; Gratch, S.; Kincaid, J. F.; Spell, A.; Stroupe, J. D. *J. Am. Chem. Soc.* **1958**, *80*, 1768.
(5) Karasz, F. E.; O'Reilly, J. M. *Rev. Sci. Instrum.* **1966**, *37*, 255.
(6) Sochava, I. V.; Trapeznikova, O. N. *Vestn. Leningr. Univ. Ser. Fiz. Khim.* **1958**, *13*, 65.
(7) McCrum, G.; Read, B. E.; Williams, G. "Anelastic Processes in Polymers"; Wiley: New York, 1967.
(8) Slichter, W. P. *NMR Basic Princ. Prog.* **1971**, *4*, 209–231.
(9) O'Reilly, J. M.; Karasz, F. E. *J. Polym. Sci., Part C* **1966**, *14*, 49.
(10) Wittman, J.; Kovacs, A. J. *J. Polym. Sci., Part C* **1975**, *16*, 4443.
(11) Roe, J. M.; Simha, Robert. *Int. J. Polym. Mater.* **1975**, *3*, 193.
(12) Sharanov, Y. A.; Volkenstein, M. V. *Solid State Phys.* **1963**, *5*, 590.
(13) Petrie, S. E. B.; Marshall, A. K. *J. Appl. Phys.* **1975**, *46*, 4223.
(14) O'Reilly, J. M.; Karasz, F. E. *Polym. Prepr., Am. Chem. Soc., Div. Polym. Sci.* **1964**, *5* (2), 351.
(15) Beatty, C. L.; Karasz, F. E. *Org. Coat. Plast.* **1975**, *35*, 370.
(16) Beck, D. L.; Hiltz, A. A.; Knox, J. R. *SPE Trans.* **1963**, *3*, 1.
(17) Hellwege, K. H.; Hennig, J.; Knappe, W. *Kolloid Z. Z. Polym.* **1962**, *186*, 29.
(18) Kusy, R. P. *J. Polym. Sci., Polym. Chem. Ed.* **1976**, *14*, 1527.
(19) Sundararajan, P. R.; Flory, P. J. *J. Am. Chem. Soc.* **1974**, *96*, 5025.
(20) Tonelli, A. E., private communication.
(21) O'Reilly, J. M.; Mosher, R. A. *Macromolecules* **1981**, *14*, 602.
(22) Goldstein, M. *J. Chem. Phys.* **1976**, *64*, 4767.
(23) Chang, S. S.; Bestul, P. B. *J. Chem. Phys.* **1972**, *56*, 503.

Stability of the Cross-Linked Tropomyosin Dimer: Cross-Link Effect on the Cooperativity of the Ordering Process and on the Maximum in the Helix Probability Profile

Wayne L. Mattice* and Jeffrey Skolnick†

Department of Chemistry, Louisiana State University, Baton Rouge, Louisiana 70803.
Received December 11, 1981

ABSTRACT: A configuration partition function has been formulated for a partially helical, cross-linked, in-register dimer composed of polypeptide chains of identical degree of polymerization. The three important features incorporated in this formulation are as follows: (1) Conformational flexibility is allowed in the cross-linking unit, with certain of the cross-link configurations giving rise to nonalignment of helices propagating away from the cross-link site. (2) Cross-linking of the helices may be accompanied by deformation of the helices near the cross-link site (or may induce stress in the cross-linking unit). (3) There is assumed to be a vanishingly small probability that a sequence of random coil residues connecting two helical segments will adopt a configuration that causes the helical segments to be collinear. Application is made to the case of cross-linked α-tropomyosin. Features 1 and 2, which are indistinguishable in this formulation of the configuration partition function, are found to have a profound impact on the high-temperature portion of the thermal denaturation of the cross-linked dimer. Feature 3 has two important consequences for the helix probability profile in the middle of the thermal denaturation: local detail, seen at low helicity, is obscured, and the maximum in the helix probability profile is shifted to the residue at the cross-link site. Thus conclusions as to the most stable helical region in the cross-linked dimer will be affected by the incorporation of feature 3 into the configuration partition function.

Dimeric tropomysin has a helical content greater than 90% in physiological media at low temperatures.[1-7] Helix–coil transition theory indicates that monomeric tropomyosin at low temperature should have a helical content in the vicinity of 17%.[8] A logical inference is that helix–helix interaction constitutes the major factor responsible for the high helicity of the dimeric form.[9-12] This extra stabilization can be overcome by an appropriate increase in temperature, as is shown by the observation of thermal denaturation for the cross-linked dimer of tropomyosin.[4,5] These features of the behavior of tropomyosin have been rationalized by a theoretical treatment of the helix–coil transition in in-register, two-chain, coiled-coil polypeptides that may or may not be cross-linked.[13] The objective here is to explore consequences of several refinements in the theoretical treatment, with special emphasis on their implications for the thermal denaturation of cross-linked tropomyosin.

Pertinent aspects of the original treatment are conveniently presented with the aid of schematics A and B of Figure 1. Figure 1A schematically depicts two identical helical chains cross-linked via a disulfide bond. Helices, which are depicted as thin rods, are parallel and in register. Separation of the two helices is assumed to be so small that residue i in one chain interacts with residue i on the other chain. This interaction is represented by the dashed line drawn for the residue denoted by the arrow to its partner on the other chain. Figure 1B depicts a configuration in which the tail of one chain is in the random coil state. It is assumed that the disordered segment does not interact with the other polypeptide chain. We now focus on contributions made to the statistical weight of each configu-

† Present address: Department of Chemistry, Washington University, St. Louis, MO 63130.

0024-9297/82/2215-1088$01.25/0